



ELSEVIER

Available online at www.sciencedirect.com



Computer Communications xxx (2006) xxx–xxx

---



---

**computer**  
 communications
 

---



---

www.elsevier.com/locate/comcom

## Traffic engineering with OSPF-TE and RSVP-TE: Flooding reduction techniques and evaluation of processing cost

Stefano Salsano <sup>a,\*</sup>, Alessio Botta <sup>b</sup>, Paola Iovanna <sup>c</sup>, Marco Intermite <sup>b</sup>, Andrea Polidoro <sup>a</sup>

<sup>a</sup> *DIE – Università di Roma “Tor Vergata,” Dip. Ingegneria Elettronica Via di Tor Vergata 110, 00133 Rome, Italy*

<sup>b</sup> *CoRiTeL – Consorzio di Ricerca sulle Telecomunicazioni*

<sup>c</sup> *Ericsson Lab Italy S.p.A.*

Received 11 July 2003; received in revised form 6 December 2005; accepted 7 December 2005

### Abstract

This paper considers two important aspects related to the control plane of Traffic Engineered IP/MPLS networks: the “flooding reduction” mechanisms and the evaluation of processing cost for signaling and routing protocols. The flooding reduction mechanisms are needed to reduce the amount of information exchanged by Traffic Engineering enabled routing protocols. The trade-off between the amount of information exchanged and the network performance (connection blocking probability) is discussed in the light of specific aspects of OSPF-TE routing protocol and RSVP-TE signaling protocol. Different mechanisms are analyzed and a suggestion is given for the best one. The dynamic aspects related to the time needed to distribute the routing and signaling information are considered. Finally, the combined processing cost of routing and signaling is analyzed, and the possible bottlenecks of the architecture are discussed. It is worth mentioning that the discussed results have been derived not only with simulation/analysis but also with measurements coming from a testbed implementation.

© 2005 Elsevier B.V. All rights reserved.

*Keywords:* MPLS traffic engineering; OSPF-TE; RSVP-TE

### 1. Introduction

The so-called “new generation networks” handle a huge amount of IP traffic, a large portion of this traffic demands more than “best effort” service (for example QoS and reliability). Multi-Protocol Label Switching (MPLS) technology [1] can be useful to cope with these requirements. MPLS can enable smart Traffic Engineering (TE) [2,3] strategies, which handle in the most flexible way the network resources, and react dynamically to traffic changes. In this advanced scenario, paths for traffic flows can be chosen according to some optimality criteria by the so-called Constraint Based Routing (CBR) algorithm. The input to the CBR algorithm is the information about the status of the network that is distributed in real-time by the routing protocol. The paths are

dynamically setup and released by means of a proper signaling protocol. Each MPLS-TE enabled node supports both a routing protocol and a label distribution protocol. The possible routing protocols are OSPF-TE [4] and ISIS-TE [5], which extend OSPF and IS-IS respectively. Specifically, the traditional routing protocols have been enhanced with the ability to carry information related to link attributes/states, to be used for explicit route calculation (e.g., available/reserved bandwidth). The label distribution protocol (or “signaling” protocol) is used to setup the so called Label Switched Paths (LSPs), supporting both explicit route indication and reservation of resources during dynamic LSP setup. RSVP-TE [6] and CR-LDP [7] are the two “TE-capable” label distribution protocols. In the following we will always consider OSPF-TE as the routing protocol and RSVP-TE as the signaling/label distribution protocol. This is consistent with the decisions in IETF to continue with the standardization of RSVP-TE rather than CR-LDP [8]. Fig. 1 provides a representation of the logical entities involved in the TE pro-

\* Corresponding author. Tel.: +39 06 7259 7450; fax: +39 06 7259 7435.  
*E-mail address:* stefano.salsano@uniroma2.it (S. Salsano).

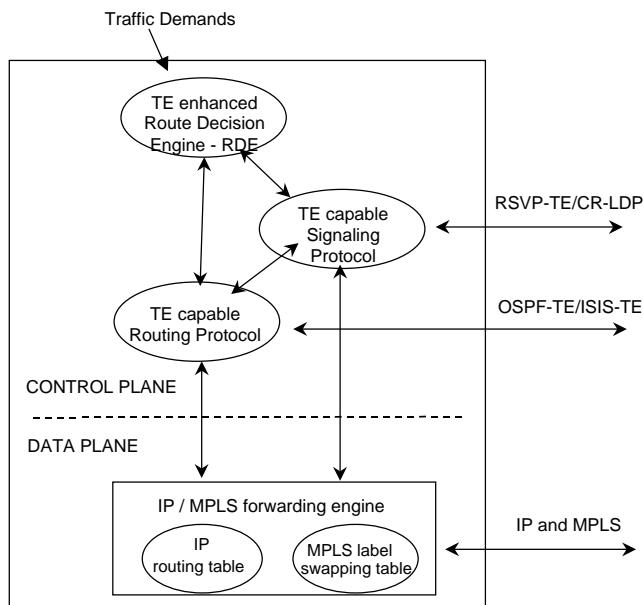


Fig. 1. Architecture of a TE enabled node (LER case).

This can be accomplished either with a static set of thresholds or with “dynamic” thresholds, by considering the relative variation with respect to the older information. We compare these two approaches, showing that the dynamic approach performs slightly better than the fixed thresholds approach and it is much easier to manage and tune. We will show that these mechanisms can reduce the amount of flooding in a network by a large factor (e.g., by 5 or 10 times).

After presenting the network and traffic models in Section 2, in Section 3 we will analyze the performance in terms of call blocking probability covering the trade-off between signaling load and performance. Our results are consistent to those described in the literature ([9–11]) but we introduce noteworthy contributions:

- the analysis of why the dynamic thresholds are preferable to the static one and the refinements of the static thresholds to reach the performance of the dynamic ones
- results coming both from simulation and from a testbed implementation with real measurements.

We observe that the traffic engineering process described so far is a highly distributed process, which can suffer of inconsistent co-ordination between the various elements. There are two possible sources of inconsistency that should be taken into account: the “*Information Propagation Time*” and the “*Imprecise Information*”.

The *Propagation Time* problem is related to the time needed to propagate the information in the network via signaling and routing protocols. In the mean time when the information is not up-to-date, an Edge Node can take incorrect (or sub-optimal) route selection decision. Another similar problem is related to the race conditions between allocation requests coming from two different Edge Nodes and arriving to an internal node almost in the same time, when resources are not enough to accommodate both. Note that in the design of the control architecture the network architect has few chances to solve this kind of problems, which are inherent to the distributed approach. Nevertheless, it is important to evaluate their impact on the performance of the network.

The *Imprecise Information* problem is related to the “reduced” information that can be distributed using OSPF-TE. Due to the “flooding reduction”, the information available in the Edge Nodes to take routing decisions will be an approximation of the actual resource status. The impact of this approximation on network performance (e.g., network utilization, call blocking probability) must be evaluated. Note that the network architect has greater control on these aspects, as there are several flooding reduction techniques that can be chosen (and then tuned). A trade-off can be envisaged between the signaling load to distribute the information and the performance in terms of network utilization and call blocking probability.

Some works in the literature describe the problem of Imprecise Information and analyze the network performance. The work in [9] focuses on the trade-off between

cess and of their relationships (including the “data plane” elements).

We assume that Edge Nodes (LER – Label Edge Routers) receive the indication of the “Traffic Demands” to be supported, and that this is a dynamic process. Note that in this context a Traffic Demand (i.e., a *flow*) is typically an *aggregate* of several IP micro-flows. Once a request has been presented to an Edge Node, we assume that a logical entity, that will be referred to as “Route Decision Engine” (RDE), chooses the proper route within the network.<sup>1</sup> The RDE gathers the information related to the current topology and resource usage in the network by continuous interaction with the TE capable routing protocol (OSPF-TE in our assumption). When the RDE has chosen the route for a Traffic Demand, the corresponding LSP will be setup using RSVP-TE protocol, which will take care of performing node-by-node admission control and actual resource allocation. OSPF-TE advertises the change of local resource allocation status to all other LSRs by sending a Link State Update (LSU) message containing a special kind of Link State Advertisement (LSA) object called *opaque LSA* [8]. The object is called opaque because it is “hidden” to the basic OSPF routing logic, as it is only used by the TE logic. The LSU message is distributed to all LSRs using the OSPF “flooding” procedure. In order to avoid that the information flooding is executed for each minimal change, some “flooding reduction” mechanisms need to be used, so that the origination rate of OSPF-TE LSU messages can be reduced.

The basic method to address the signaling flooding problem is the distribution of a “coarser” link-state information.

<sup>1</sup> Note that the Route Decision Engine (RDE) is a logical process, from the physical standpoint it can either run “on” the LER or it can run on a separate machine connected to the edge node.

143 the amount of flooding and the network performance in  
 144 terms of utilization/blocking probability. The aspects of  
 145 processing cost are not explicitly dealt with. In [10], a sim-  
 146 ilar evaluation on the trade-off is given and some process-  
 147 ing cost aspects are also considered ([11] further  
 148 investigates on the processing cost aspect). The analysis  
 149 of processing cost in these works is concentrated on the  
 150 routing protocol aspects and on the calculation of CBR  
 151 algorithms. The processing cost related to the signaling  
 152 protocol for path setup is not considered. We believe that  
 153 this cost cannot be neglected and an important contribu-  
 154 tion of our work is the combined evaluation of processing  
 155 cost for routing and signaling protocols given in section 0.  
 156 Note that the work in [9–11] was based on generic assump-  
 157 tions regarding TE-enhanced routing and signaling proto-  
 158 cols, as the protocols were not yet defined. In this paper  
 159 we could consider the actual behavior of OSPF-TE,  
 160 RSVP-TE and their interaction and even provide results  
 161 coming from a testbed implementation. To conclude the  
 162 survey on relevant literature, a very detailed analysis of  
 163 processing cost for OSPF-TE has been performed in [13],  
 164 anyway the focus of that work was on the stability issues  
 165 of OSPF and the results cannot be applied in our context.  
 166 To the best of our knowledge, the issue of Propagation  
 167 Time, i.e., the impact of the short-term dynamics of OSPF-  
 168 TE and RSVP-TE has not been thoroughly analyzed  
 169 before, and this constitutes a second important novelty of  
 170 our work, reported in Section 4. The goal is to define the  
 171 operational range where there is no impact of this inconsis-  
 172 tency on the network operations.

## 173 2. Network and traffic models

### 174 2.1. Network model

175 Two different network topologies have been considered  
 176 for our study (Fig. 2). Table 1 reports the number of nodes  
 177  $N$ , the number of unidirectional links  $L$ , the hop count

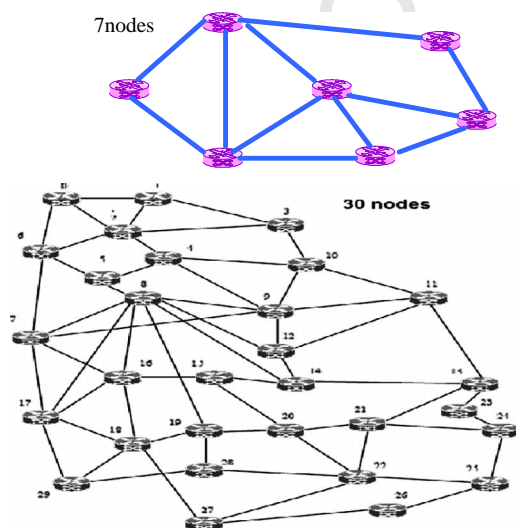


Fig. 2. Network topologies.

Table 1  
Network topologies

Topology	$N$	$L$	$\bar{h}$	$C$ (Mb/s)
7nodes	7	44	1.52	100
30nodes	30	118	3.96	635

averaged among all node pairs  $\bar{h}$  and the link capacity  $C$  (Mb/s). The reason to have two different topologies is that the smaller 7nodes topology could be implemented both in the simulation study and in a testbed (see II. C below), allowing to compare simulation results with real measurements. The 30nodes topology (the same used in [12]) was used to have simulation results for a network size comparable with a real life scenario.

### 2.2. Traffic model and CBR algorithm

In order to model the offered traffic, we considered two different traffic models, a “uniform” model and a “non-uniform” one.

We denote every (source, destination) couple as a Traffic Relation, the arrival rate of Traffic Demands within each Traffic Relation  $i$  is denoted as  $\lambda_i$  ( $s^{-1}$ ). Under the uniform model, each node generates traffic requests directed to all other nodes of the network, according to a Poisson process, with uniform random selection of destination nodes, therefore  $\lambda_i = \lambda \forall i$ . The total arrival rate of Traffic Demands originating in each node is denoted as  $\lambda_{node} = (N - 1)\lambda$ .

In the case of “non-uniform” model, the composition of two request arrival processes is considered. In addition to a background uniform traffic, of rate  $\lambda_{BG}$  ( $s^{-1}$ ) per each traffic relation, we have a foreground traffic generated by a number of hot-spot pairs, with rate  $\lambda_{FG}$  ( $s^{-1}$ ). According to [10], we varied the amount of this foreground traffic in respect of total offered load up to 30%.

We model connection holding times using a negative exponential distribution where  $T$  is the mean holding time. The bandwidth of each Traffic Demand is uniformly distributed between 0 and  $2b$  of the capacity  $C$  of a link. Therefore, the mean value of a single Traffic Demand is  $bC$ . The offered load for each traffic relation  $i$  will be  $R_o^i = \lambda_i T b C$  (bit/s). In the simulation scenario used in this paper we set  $T = 200$  s (a relatively short flow duration in order to have a quite dynamic scenario).

In order to characterize the offered load to the network, we define a “normalized” offered load assuming that all the traffic demands are routed through a shortest path. We denote  $h_i$  the shortest path length of the traffic relation  $i$ , hence the normalized offered load becomes ( $N_{TR}$  is the number of Traffic Relations):

$$\rho_{SP} = \sum_{i=1}^{N_{TR}} R_o^i h_i / \sum_{j=1}^L C_j. \quad 222$$

In the “uniform” traffic model the normalized traffic load becomes, as  $N_{TR} = N(N - 1)$ :  
 223  
 224

$$\rho_{SP} = \sum_{i=1}^{N_{TR}} \lambda T b \bar{h} / L = N(N-1) \lambda T b \bar{h} / L.$$

where  $\bar{h}$  is the mean distance (in number of hops) between nodes, averaged across all traffic relations (i.e., all pairs of Edge Nodes).

In the non-uniform model we can divide the total offered load in the two background and foreground components:

$$\rho_{SP} = \sum_{i=1}^{N_{TR}} \lambda_{BG} T b \bar{h} / L + \sum_{i=1}^{N_{HOT-SPOT}} \lambda_{FG} T b h_i / L$$

We considered a CBR algorithms. that favors an evenly distribution of the traffic in the network even if it means considering longer path (“least resistance” [14]). The cost  $S_i$  of each link  $i$  is  $S_i = B_T / B_i^A$  where  $B^T$  is the maximum link bandwidth in the network, and  $B_i^A$  is the available bandwidth in the link  $i$ . Links with not enough bandwidth are pruned as well.

### 2.3. Simulation environment and testbed

We implemented a “custom” event-based simulator for the OSPF-TE/RSVP-TE environment. The simulator is developed in C++ under the Linux OS, and is available at [15]. The simulator is able to consider two different scenarios. In the first one there is the assumption of “ideal” (e.g., instantaneous) propagation of RSVP-TE and OSPF-TE information (see results in section 3). In the second scenario the real propagation of OSPF-TE and RSVP-TE information (see results in Section 4) is considered in the simulation by taking into account the processing and transmission time of RSVP-TE and OSPF-TE messages.

The testbed is composed of 7 PCs with a Linux Operating System (RedHat 7.1), which are interconnected by point-to-point Ethernet links (100 Mb/s) according to the topology shown in Fig. 2 (7nodes topology). Each PC represents a network node with a fully functional implementation of the MPLS-TE control plane (including OSPF-TE and RSVP-TE daemons, Route Decision Engine, Traffic Request Generator). The software packages installed and active on the test bed are: MPLS provided by Sourceforge [16], RSVP-TE daemon from TEQUILA project [17] and OSPF daemon by GNU Zebra software, version 0.92 [18] patched with TE extensions. It implements OSPF v.2 according to [19] with Opaque LSA capabilities [20]. Additional details on the testbed can be found in [21,22].

### 3. “Resource thresholds” mechanisms

The idea of resource threshold mechanisms is to advertise only significant changes of link state information. Therefore, a single advertisement is typically performed after a number of LSP setups and releases, instead of communicating the change of network status for each setup (release) of an LSP. The threshold mechanisms can be classified in static and dynamic ones.

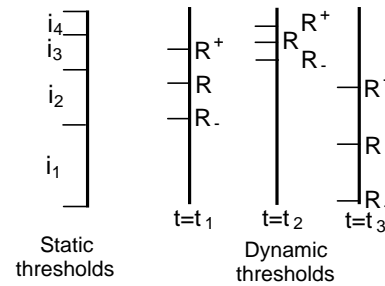


Fig. 3. Static and dynamic thresholds.

Using static thresholds, the link capacity is divided in intervals, limited by upper and lower threshold levels. In order to limit the effect of the inaccuracy introduced by the thresholds, it is sensible to fix just a few threshold levels in the lower part of link bandwidth occupancy and much more levels in the higher part of link bandwidth occupancy (near congestion). There is a large degree of freedom in the choice of the number and of the values of the threshold levels. In order to experiment with the different choices it is reasonable to define families of static threshold mechanisms that can be characterized by few parameters. The two families of threshold mechanisms (“logarithmic” and “3-piece-linear”) that we have considered are described in Appendix A. Additional details about the use of threshold values are given in Appendix B.

The dynamic threshold approach assigns an initial threshold level on the empty link and calculates next upper and lower levels as functions of currently advertised reservation amount. Let  $C$  be the link capacity and  $R$  the currently advertised reserved bandwidth, the upper and lower thresholds are calculated, respectively, as

$$R^+ = R + F \cdot (C - R); \quad R^- = R - F \cdot (C - R).$$

Note that, as desired, the difference between upper and lower thresholds becomes narrower when the available bandwidth decreases. Note also that a larger value of  $F$  ( $0 < F < 1$ ) means more spaced dynamic threshold levels and a coarser vision of network status in the RDEs. Fig. 3 provides a sketch of the two mechanisms.

#### 3.1. Results and discussion

Let us analyze the trade-off between the amount of flooding and the network performance in terms of connection blocking. We started with a simulation analysis, in the scenario of “ideal” (e.g., instantaneous) propagation of RSVP-TE and OSPF-TE information.

The main results are reported in Figs. 3–6.<sup>2</sup> The leftmost value of the curves represents the network behavior with no threshold mechanisms (perfect vision). When we have a coarser information (smaller number of thresholds in the

<sup>2</sup> 30nodes topology,  $b=0.05$ ; for the static thresholds: logarithmic function  $\alpha = 10^4$ . The figures are obtained under the uniform traffic model, but no difference can be noticed under the non-uniform traffic model.

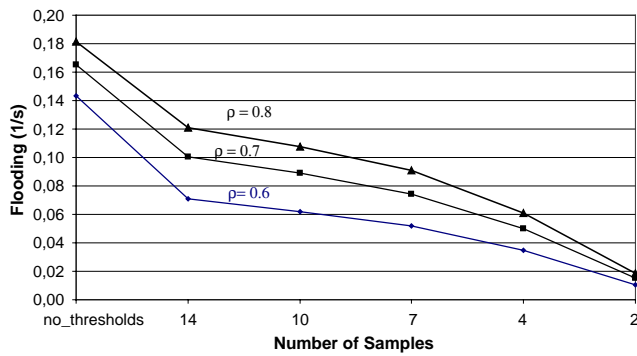


Fig. 4. Static thresholds: flooding.

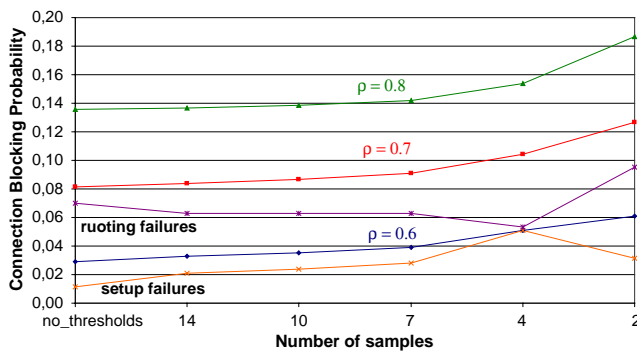


Fig. 5. Static thresholds: connection blocking probability.

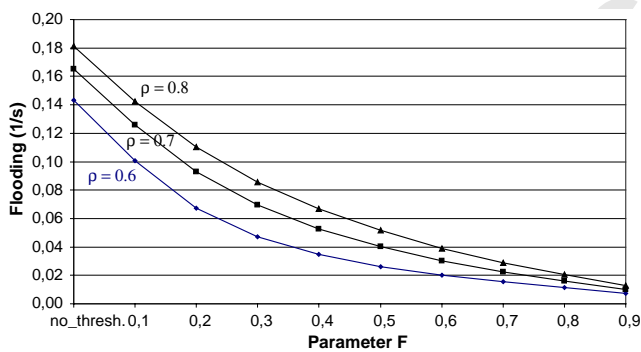


Fig. 6. Dynamic thresholds: flooding.

Looking at Figs. 3–6, we observe that there is a region (starting from the left) where the blocking probability does not increase significantly while the OSPF-TE message flooding is greatly reduced. This suggests that the optimal working point is where the blocking probability start to increase: in the given scenarios 7 thresholds for the static thresholds or  $F = 0.7$  for the dynamic ones.

We define as “merit” factor the ratio between the amount of flooding with thresholds and without thresholds. For offered load 0.6, this factor is 3.1 for static-threshold and 10.6 for the dynamic thresholds, respectively at 7 thresholds and at  $F = 0.7$  where the blocking probability is still under control. In Fig. 8 we compare 3-piece linear ( $\beta = 0.75$ ,  $\gamma = 0.95$ ) static thresholds with 14 and 7 levels, logarithmic ( $\alpha = 10^4$ ) static thresholds with 14 and 7 levels and dynamic ( $F = 0.7$ ) thresholds. The 3-piece linear and the logarithmic thresholds have the same merit factor (1.7) for 14 levels while the 3-piece linear yields a larger reduction (merit factor 3.3) than the logarithmic (2.2) for 7 levels. The dynamic thresholds have the larger merit factor (7.3). Note that the connection blocking probability using static mechanisms with 14 thresholds is unchanged with respect to the case without any threshold method, and only minimally increased using static mechanism with 7 thresholds or dynamic mechanisms with  $F = 0.7$ .

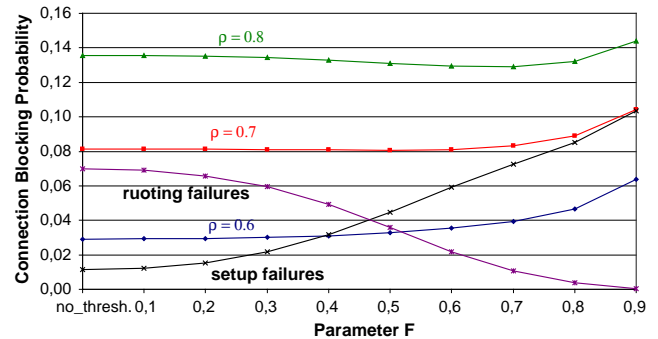


Fig. 7. Dynamic thresholds: connection blocking prob.

static scenario, larger  $F$  in the dynamic one) we can drastically reduce the amount of flooding (the number of LSU messages originated per link per second is shown). On the other hand, blocking probability starts to increase when the information is too coarse. The analysis is reported for three different values of the “conventional” offered load  $\rho_{SP}$  from 0.6 up to 0.8. The typical operating point should be  $\rho_{SP} = 0.6$  or less, where the blocking probability is around 2%, while  $\rho_{SP} = 0.7$  and  $\rho_{SP} = 0.8$  can be already considered overload conditions, considering that the blocking probability is respectively in the order of 8% and 14%. Note that we will not show 95% confidence intervals of simulation results, however results are averages over long runs and such confidence intervals are always smaller than 3% of the value.

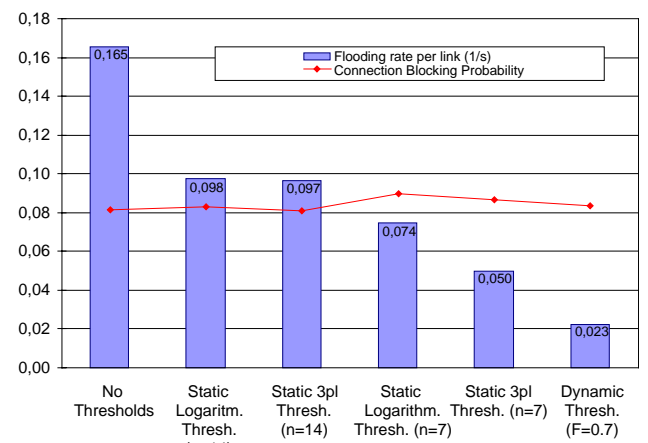


Fig. 8. Static vs. dynamic threshold.

329  
330  
331  
332  
333  
334  
335  
336  
337  
338  
339  
340  
341  
342  
343  
344  
345  
346  
347  
348  
349  
350  
351  
352  
353  
359  
360  
361  
362  
363

364 Several simulations have been carried out for the two  
 365 considered network topologies, under different load scenar-  
 366 ios and different traffic models: using the dynamic thresh-  
 367 olds with  $F=0.7$ , we obtained a merit factor ranging  
 368 from 8 to 15 without affecting in significant way the net-  
 369 work performance (same blocking probability). The results  
 370 with static thresholds are not equally stable. Comparing  
 371 the static thresholds with the dynamic ones, we think that  
 372 it is much easier to reduce OSPF-TE protocol message  
 373 exchange with the dynamic ones. Moreover, we can say  
 374 that the dynamic threshold mechanism is simpler to be con-  
 375 figured because only the value of  $F$  needs to be fixed. This  
 376 means that one does not have to configure all the threshold  
 377 values in the routers as in the static thresholds. The use of  
 378 dynamic thresholds could represent an important improve-  
 379 ment with respect to the currently used static thresholds.

380 In order to validate the simulation analysis, the dynamic  
 381 threshold mechanism has been implemented in our testbed  
 382 and various experiments have been carried out in parallel  
 383 with the simulation environment with the *7nodes* topology  
 384 (identical to the testbed topology). The main results are  
 385 reported in Figs. 9 and 10. These two figures represent a  
 386 comparison between the simulated scenario and the emu-  
 387 lated one (testbed). An offered load  $\rho_{SP} = 0.7$  is used. As  
 388 can be seen from the figures we have obtained in the test-  
 389 bed the same behavior as in the simulation.

390 The final consideration in this section concerns the sig-  
 391 naling load due to RSVP-TE. In Figs. 5 and 7 the block-

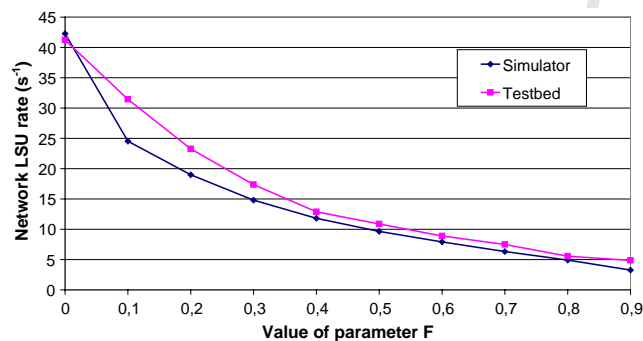


Fig. 9. Flooding reduction comparison.

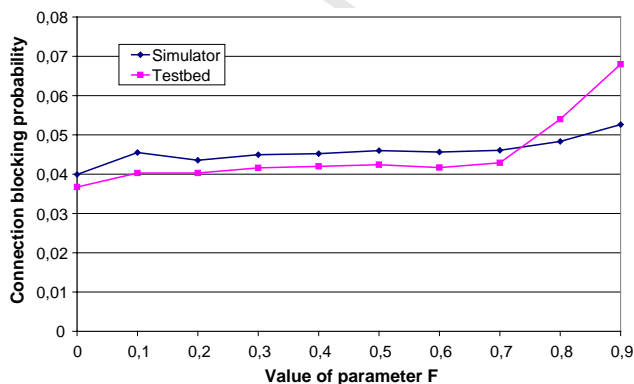


Fig. 10. Blocking probability comparison.

ing probability for an offered load  $\rho_{SP} = 0.7$  is split into  
 the two components of “routing” failures and “setup”  
 failures. The former ones represent the connections reject-  
 ed by the CBR algorithm in the ingress Edge Node, the  
 latter ones the connections which are accepted by the  
 CBR algorithm, but then rejected by the RSVP-TE setup  
 procedure due to the local admission control in one of the  
 crossed nodes. According also to [9], we note that the  
 coarser the information, the larger the number of connec-  
 tions that are rejected during the setup phase, originating  
 an unneeded signaling in the network. This suggests that a  
 more detailed analysis should be performed to take into  
 account also the signaling load in the definition of the  
 optimal working point. This analysis will be carried out  
 in Section 0.

#### 4. Impact of message processing/transmission time

As we have observed in the previous section, there is a  
 good agreement between the results coming from the “ideal”  
 simulator and from the testbed. We recall that in the  
 simulations analyzed in the previous section, an ideal  
 behavior for both reservation and routing protocol has  
 been assumed. This means that all processing and propaga-  
 tion times of control plane messages were considered to be  
 null.

The agreement between simulation and testbed results  
 seems to imply that there is no impact of the RSVP-TE  
 and OSPF-TE delays in propagating signaling messages.  
 In this paragraph, we want to verify under which operating  
 conditions this assumption is valid. To analyze the impact  
 on network performance of RSVP-TE and OSPF-TE  
 delays, as a function of the overall connection requests  
 rate, we introduced the processing delays in the simulator  
 and considered the actual behavior of RSVP-TE and  
 OSPF-TE in propagating their messages.

As a preliminary step, we had to figure out the charac-  
 teristic delays of RSVP-TE and OSPF-TE messages. The  
 value for the processing/propagation time of an OSPF-  
 TE LSU has been taken from [23]. Our simplifying hypoth-  
 esis is that this delay remains constant from hop to hop and  
 over time. Therefore, the propagation time of an LSU  
 flooding procedure is linear with the number of hops  
 crossed. The value of a single hop processing/propagation  
 time has been set to 34 ms.

RSVP-TE messages (Path, Resv, PathTear, and Resv-  
 Tear) processing/propagation times were taken from [24].  
 Again, we made the simplifying assumption that all these  
 times remain constant during the evolution of a simulation,  
 as if they were independent from the number of reservation  
 sessions installed. We considered values of 14, 14, 6, and  
 20 ms respectively for Path, Resv, PathTear, and ResvTear  
 processing/propagation times.

These delays add inaccuracy in the RDE vision of net-  
 work status. Each router will have a different vision of  
 the status of network occupation, and this vision in general  
 is not aligned with the real one. Similarly to the effect of a

392  
393  
394  
395  
396  
397  
398  
399  
400  
401  
402  
403  
404  
405  
406  
407  
408  
409  
410  
411  
412  
413  
414  
415  
416  
417  
418  
419  
420  
421  
422  
423  
424  
425  
426  
427  
428  
429  
430  
431  
432  
433  
434  
435  
436  
437  
438  
439  
440  
441  
442  
443  
444  
445  
446

447 threshold mechanism this will cause the RDE not to always  
448 select the optimal paths for LSPs.

449 By means of simulations, we analyzed the impact of the  
450 inaccuracy on network performance. A scenario with no  
451 thresholds is analyzed, in order to consider this phenome-  
452 non in isolation, the load  $\rho_{SP}$  is 0.7. Under the typical sce-  
453 nario assumed so far, with the total requests arrival rate  
454  $\lambda_{node}$  of  $0.07 \text{ s}^{-1}$ , we noticed no impact of processing/trans-  
455 mission delays. Therefore, we started to increase the rate of  
456 incoming LSP requests in the network. To have a fair com-  
457 parison, we kept the network load constant, therefore we  
458 reduced the connection holding time. We were able to  
459 understand when the considered delays start to be influent  
460 on network performance. Fig. 11 reports the connection  
461 blocking probability and setup failures versus the total  
462 arrival rate for the “ideal” system and the system with pro-  
463 cessing/transmission delays. The blocking probability of  
464 the ideal system is obviously not dependent on the arrival  
465 rate. It can be seen that RSVP-TE and OSPF-TE messages  
466 delays start to influence the connection blocking probabili-  
467 ty in the system with processing/transmission delays when  
468 the request rate is increased by a factor of 20. The degrada-  
469 tion of connection blocking is relatively mild, considering  
470 that for an increase of request rate by a factor of 100, it  
471 goes from 8% to 9.5%. On the other hand, the inaccurate  
472 vision of network status causes a rapid growth of setup fail-  
473 ures, which are almost null in our initial scenario with  $\lambda_{node}$   
474 of  $0.07 \text{ s}^{-1}$ . When  $\lambda_{node}$  is 20 times higher ( $\sim 1.4 \text{ s}^{-1}$ ), the  
475 setup failures are in the order of 3% of offered calls.

476 In order to understand the previous results, consider  
477 that a node is concerned by a connection when it is source,  
478 destination or in the path of an LSP. Let  $f_{node}$  be the arrival  
479 rate of Traffic Demands that “concern” a node:  
480  $f_{node} = \lambda_{node} \cdot (\bar{h} + 1)$ , where  $\bar{h}$  is the mean length of LSPs  
481 that are setup (the blocking probability is neglected).  $1/f_{node}$   
482 will be the mean inter-arrival time of two connections  
483 that concern a node. Approximating  $\bar{h}$  with the shortest  
484 path, we have that  $1/f_{node} = 3.25 \text{ s}$  for  $\lambda_{node} = 0.07 \text{ s}^{-1}$ .  
485 According to the assumed values, the characteristic times  
486 of RSVP-TE and OSPF-TE procedures are in the order  
487 of 50–100 ms, that is 30–60 times smaller than the consid-

ered value of  $1/f_{node}$ . The impact on blocking probability  
starts when the inter-arrival time of calls concerning a node  
is in the order of the characteristic times of routing and sig-  
naling procedures.

## 5. Combined routing/signaling processing cost

In this section, we evaluate the processing cost of the  
combined OSPF-TE/RSVP-TE architecture. We will show  
that threshold mechanisms are effective in decreasing the  
load component due to OSPF-TE, and that the RSVP-  
TE processing load must be carefully considered as it con-  
stitutes the system bottleneck.

The evaluation is based on the definition of a theoretical  
model of processing costs, combined with the simulator  
environment. Using our simulator, we can evaluate the  
number (and the rate) of OSPF-TE flooding procedures  
that are started by a node. We can also count the number  
of RSVP-TE messages (Path, Resv, PathTear, and Resv-  
Tear). Then we are able to evaluate the total processing  
cost by multiplying the processing cost of each message  
 $w_{msg}$  for its rate  $r_{msg}$ .

We will also confirm the theoretic/simulation model  
results with measurements performed in the tested, related  
to message rates and to the CPU load.

### 5.1. Message processing cost

Let us consider the different components of processing  
cost in a TE enabled MPLS network. A component is relat-  
ed to the OSPF-TE messages due to the flooding of state  
information. Another component is the processing cost of  
the LSP setup (and release) messages via RSVP-TE proto-  
col. Due to the soft state approach, the processing related  
to RSVP refresh messages must be also considered.

The processing cost for each message obviously depends  
on the specific implementation of OSPF-TE and RSVP-  
TE. In general it can be dependent on the network topolo-  
gy (e.g., on the size of the network) and on the network sta-  
tus (e.g., number of established LSPs). In order to perform  
our evaluation what we need is actually the relative pro-  
cessing cost of the messages, rather than their absolute val-  
ues. For this purpose, we take as reference the processing  
cost of an OSPF Link Status Update (LSU) message con-  
taining the first copy of a Link State Advertisement (LSA)  
received by a router. We assume that one unit of processing  
cost is needed to check that the LSA is not yet “installed”  
in the database, to install it and to prepare a copy of it to  
be sent to all other interfaces but the receiving one. We can  
now in general define the processing cost of the other mes-  
sages with reference to this processing unit, using a set of  
generic parameters as shown in the third column of Table  
2. For example  $a_1$  is the relative processing cost of a  
“Copy-LSA” message with respect to the “First-LSA mes-  
sage. The processing cost of RSVP-TE messages is actually  
split into two factors,  $Q$  and  $b_i$ ,  $i = 1-5$  for the different  
RSVP-TE messages.  $Q$  represents the relative processing

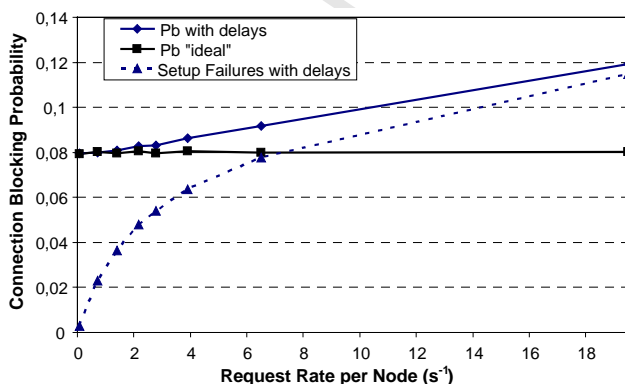


Fig. 11. Network performance vs. total request rate.

Table 2  
Control plane messages

Message	Notation	Processing unit	
		Generic	Assumed
“First-LSA”	$w_{\text{firstLSA}}$	1	1
“Copy-LSA”	$w_{\text{copyLSA}}$	$a_1$	0.5
Path	$w_{\text{Path}}$	$Q$	5
Resv	$w_{\text{Resv}}$	$Qb_1$	6
PathTear	$w_{\text{PathTear}}$	$Qb_2$	3
ResvTear	$w_{\text{ResvTear}}$	$Qb_3$	7
RefreshPath	$w_{\text{RefrPath}}$	$Qb_4$	2.5
RefreshResv	$w_{\text{RefrResv}}$	$Qb_5$	2.5

541 cost of a Path message with respect to a First LSA message:  
542  $Q = w_{\text{Path}}/w_{\text{firstLSA}}$ . The factor  $b_i$  for each RSVP-TE mes-  
543 sage represents its relative processing cost with respect to a  
544 Path message.

545 The exact parameter values are obviously dependent on  
546 the specific protocol implementations and also on the net-  
547 work operating point. For the purpose of this paper, we  
548 assumed reasonable values starting from the results avail-  
549 able in the literature. In particular, [24] have been used to  
550 infer the relative processing costs of RSVP-TE messages.  
551 [24] has been compared to [23], where the processing cost  
552 of OSPF messages is discussed, in order to estimate the val-  
553 ue of  $Q$ . The RSVP-TE processing in typical implementa-  
554 tions is dependant on the number  $n_{\text{link}}$  of active sessions  
555 per link, that can be evaluated as

$$557 n_{\text{link}} = \lambda_{\text{tot}}(1 - P_B)T \cdot \bar{h}/L.$$

558 In our scenario we have a relatively low number of  
559 active sessions per links (in the order of 20), therefore we  
560 assumed a processing cost for RSVP-TE close to the min-  
561 imum values reported in [24].

### 562 5.2. OSPF-TE and RSVP-TE message rates

563 According to the OSPF behavior, each flooding proce-  
564 dure results in the exchange of a number of LSU messages  
565 that depends on the topology of the network. For a given  
566 topology (only point-to-point links are considered) with  
567  $N$  nodes and average degree  $D$ , the number of messages  
568 that are generated by each flooding procedure is  
569  $N \cdot (D - 1) + 1$  (see Appendix C). These messages may cor-  
570 respond to two different processing costs in the node. If an  
571 (Opaque) LSA is received from a router for the first time, it  
572 has to store it and to send it to all the interfaces. When fur-  
573 ther copies of the same (Opaque) LSA are received, the  
574 node simply discards them, resulting in a lower processing  
575 cost. In particular in a flooding procedure there will be  
576  $N - 1$  “first-LSA”s and  $N \cdot (D - 2) + 2$  “copy-LSA”s.

577 Each successful LSP setup will generate a number  $h_{(x)}$  of  
578 Path and Resv messages, where  $h_{(x)}$  is the number of hops  
579 of the LSP  $x$ . The release of the same LSP will generate a  
580 number  $h_{(x)}$  of PathTear and ResvTear messages. During  
581 the lifetime of the flow the soft state nature of the LSPs will  
582 originate  $h_{(x)}$  Path and Resv messages with a rate corre-

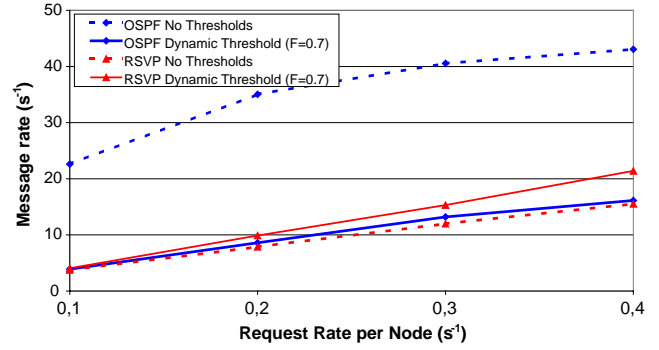


Fig. 12. Number of messages per second.

583 sponding the refresh rate  $RR$  ( $s^{-1}$ ). In the following, we  
584 will denote  $h_{\text{LSP}}$  the average number of hops of an LSP,  
585 leaving out the dependence on the specific LSP  $x$ . A failed  
586 setup of an LSP (see Fig. 13) will generate  $h_{(y)}$  Path mes-  
587 sages,  $r_{(y)}$  Resv messages up to the node where the reservation  
588 fails,  $r_{(y)}$  ResvError and ResvTear to tear down the part of  
589 the LSP attempted to set up, and  $h_{(y)} - r_{(y)}$  PathError to  
590 advertise source node about the setup failure.

591 Utilizing our testbed implementation we measured the  
592 exact number of messages exchanged among the nodes.  
593 We studied the behavior of the whole architecture in term  
594 of packets exchanged by the two protocols, OSPF-TE  
595 and RSVP-TE, comparing a scenario without any thresh-  
596 old mechanism with the one utilizing the Dynamic  
597 Thresholds with parameter  $F$  set to 0.7. Fig. 12 reports  
598 the results of these measures representing the message  
599 rate for each protocol, in both scenarios, versus the  
600 request rate per node  $\lambda_{\text{node}}$ . We can see that introducing  
601 an efficient threshold mechanism, OSPF-TE flooding is  
602 enormously reduced, while the number of RSVP messages  
603 exchanged are “lightly” increased, by the presence of the  
604 Setup Failures.

### 565 5.3. Definition of processing cost model and results

606 We started by considering the scenario where no flood-  
607 ing reduction techniques are used: a flooding procedure is  
608 executed for each state change. We consider the ideal case,  
609 where there is no delay in transmission and processing of  
610 OSPF-TE and RSVP-TE messages. Under these assump-  
611 tions, the Edge Nodes have a perfect vision of the network  
612 status and there will be no blocking at the RSVP-TE level.  
613 Let  $\lambda_{\text{tot}}$  be the total arrival rate of traffic demand to the net-  
614 work,  $P_B^{\text{CBR}}$  the blocking rate due to refusals of the CBR  
615 algorithm in the originating Edge Node and  $n_{\text{LSP}}$  the mean  
616 number of active LSP. The processing cost for this scenario  
617 is

$$618 P_{\text{tot}} = 2\lambda_{\text{tot}}(1 - P_B^{\text{CBR}})h_{\text{LSP}} \cdot (N - 1)w_{\text{firstLSA}} + 2\lambda_{\text{tot}} \\ 619 \times (1 - P_B^{\text{CBR}})h_{\text{LSP}} \cdot [N(D - 2) + 2]w_{\text{copyLSA}} + \lambda_{\text{tot}} \\ \times (1 - P_B^{\text{CBR}})h_{\text{LSP}} \cdot (w_{\text{Path}} + w_{\text{Resv}} + w_{\text{Path-Tear}} + w_{\text{Resv-Tear}}) \\ + n_{\text{LSP}} \cdot RR \cdot h_{\text{LSP}} \cdot (w_{\text{Refr-Path}} w_{\text{Refr-Resv}}).$$



620 The first two terms represent the processing load for OSPF-  
 621 TE messages: each call setup that is accepted spans on  
 622 average  $h_{LSP}$  links and on each links it triggers one flooding  
 623 procedure for the setup and one for the release; the flood-  
 624 ing procedure in turn generates  $(N - 1)$  “first” LSA mes-  
 625 sages and  $N(D - 2) + 2$  “copy” LSA messages. The third  
 626 term represents the RSVP-TE messages that are exchanged  
 627 during the successful setup and release of the LSP. The  
 628 fourth term takes into account the RSVP-TE messages  
 629 related to the maintenance of RSVP soft state: RR is the  
 630 refresh rate ( $s^{-1}$ ).

631 If we consider the scenario with flooding reduction tech-  
 632 niques and real processing and transmission times of  
 633 OSPF-TE and RSVP-TE messages, the setup of an LSP  
 634 may fail with a probability  $P_B^{RSVP}$ . The processing cost  
 635 can be represented by

$$\begin{aligned}
 P_{\text{tot}} = & 2\lambda_{\text{tot}}(1 - P_B^{\text{CBRR}})h_{LSP} \cdot \frac{1}{M} \cdot (N - 1)w_{\text{firstLSA}} + 2\lambda_{\text{tot}} \\
 & \times (1 - P_B^{\text{CBRR}})h_{LSP} \cdot \frac{1}{M} \cdot [N(D - 2) + 2]w_{\text{copyLSA}} + \lambda_{\text{tot}} \\
 & \times (1 - P_B^{\text{CBRR}})(1 - P_B^{\text{RSVP}})h_{LSP} \cdot (w_{\text{Path}} + w_{\text{Resv}} + w_{\text{PathTear}} \\
 & + w_{\text{ResvTear}}) + \lambda_{\text{tot}}(1 - P_B^{\text{CBRR}})(P_B^{\text{RSVP}})h'_{LSP} \cdot (w_{\text{Path}} \\
 & + xw_{\text{Resv}} + xw_{\text{ResvErr}} + xw_{\text{ResvTear}} + (1 - x)w_{\text{PathErr}}) \\
 & + n_{LSP} \cdot RR \cdot h_{LSP} \cdot (w_{\text{Refr-Path}} + w_{\text{Refr-Resv}}).
 \end{aligned}$$

637

638 We notice that the first two terms are reduced by the  
 639 merit factor  $M$  of the flooding reduction technique. The  
 640 term related to the RSVP load has been split into two terms  
 641 that take into account the LSPs that are successfully setup  
 642 and the LSPs that are rejected by RSVP.  $h'_{LSP}$  is the mean  
 643 length of LSPs that experience a setup failure. The param-  
 644 eter  $x$  takes into account the number of hops of the LSP  
 645 that can be setup before finding a node that rejects the  
 646 request (see Fig. 13).

647 Fig. 14 reports the total processing cost versus the  
 648 parameter  $F$  of dynamic thresholds (offered load  
 649  $\rho_{SP} = 0.7$ ,  $b = 0.05$ , NSFNET topology.). The total pro-  
 650 cessing cost is split among the routing component, the  
 651 RSVP-TE (setup and release) and the RSVP-TE refresh.  
 652 The processing cost of each message is as shown in the last  
 653 column of Table 2.

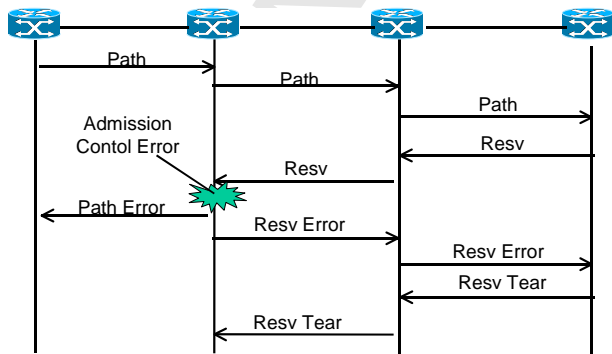


Fig. 13. Failed setup procedure.

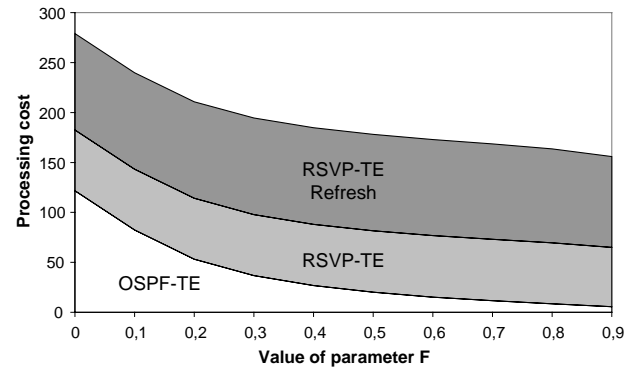


Fig. 14. Total processing cost and its components.

654 To confirm these theoretic values, we performed some  
 655 similar measurements in the testbed. We measured process-  
 656 ing load in each node in terms of percentage of CPU usage  
 657 in the two different scenarios: the first one without any  
 658 threshold mechanism (upper part of Fig. 15) and the sec-  
 659 ond one where the Dynamic Threshold mechanism is  
 660 implemented with factor  $F$  set to 0.7 (bottom part of  
 661 Fig. 15). The figures show the measured CPU processing  
 662 loads related to the two protocols (averaged on all the net-  
 663 work nodes) versus the requests arrival rate. All measure-  
 664 ments were been taken in the testbed during simulations  
 665 with network load  $\rho_{SP} = 0.7$ . The reduction of OSPF flood-  
 666 ing by means of Dynamic Threshold mechanism signifi-  
 667 cantly reduces the total processing load while the increase  
 668 of RSVP-TE load due to the presence of setup failures is  
 669 negligible.

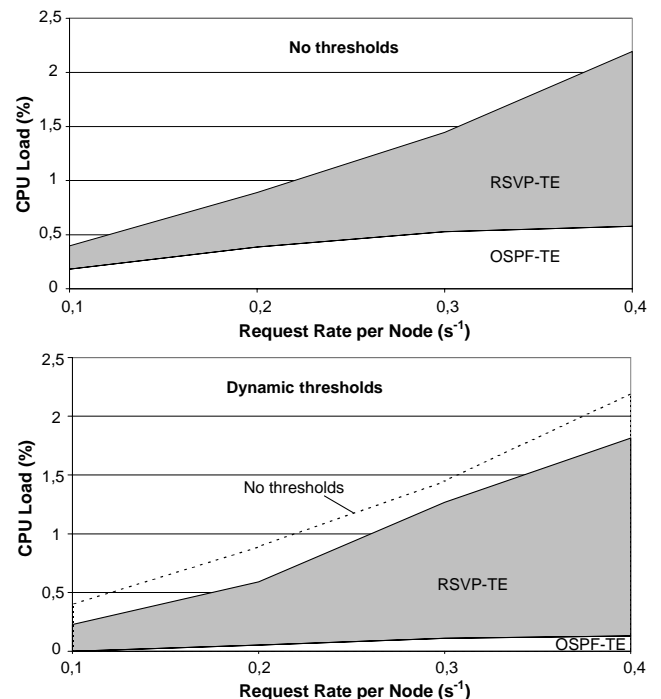


Fig. 15. Processing load.

670 The first important result is that the use of dynamic  
 671 thresholds is effective in reducing the overall processing  
 672 cost: RSVP-TE processing does not increase in a significant  
 673 way due to setup failures when the network vision become  
 674 coarser. On the other hand, the overall reduction is less  
 675 than it was expected considering the large reduction of  
 676 OSPF-TE flooding. The RSVP-TE cost component, which  
 677 is basically independent of the flooding reduction technique  
 678 (see Fig. 14), accounts for the most part of the total pro-  
 679 cessing cost in the region where these flooding reduction  
 680 techniques are effective. In particular, the RSVP-TE refresh  
 681 component has a great impact on the total processing (see  
 682 Fig. 14), suggesting that attention should be paid to reduce  
 683 it. In particular, aggregate refresh mechanisms, as well as  
 684 the reduction of refresh rate (we have considered the  
 685 default refresh rate of  $1/30 \text{ s}^{-1}$ ) could be considered. Our  
 686 analysis suggests that while total OSPF-TE processing cost  
 687 can be controlled with dynamic threshold mechanisms, the  
 688 total RSVP-TE processing cost represents a potential  
 689 bottleneck.

## 690 6. Conclusions

691 In this work, we first analyzed the effectiveness of the  
 692 flooding reduction techniques for OSPF-TE in a MPLS-  
 693 TE network. The trade-off between the amount of flooding  
 694 and the connection blocking probability has been analyzed  
 695 for different mechanisms. The result is the selection of the  
 696 dynamic threshold mechanism as the most efficient and  
 697 simplest one.

698 This analysis has been first performed assuming an  
 699 instantaneous propagation of the signaling/routing infor-  
 700 mation. Then, the transmission and processing delays of  
 701 OSPF-TE and RSVP-TE have been considered. This sec-  
 702 ond analysis was able to identify the operating conditions  
 703 under which these transmission/processing delays do not  
 704 impact on the network performance.

705 Finally, the aspects of combined processing cost for  
 706 routing and signaling have been analyzed. It is shown that  
 707 the signaling processing cost does not increase significantly  
 708 when the flooding reduction mechanism are used, therefore  
 709 the goal to reduce the overall processing cost is met. On the  
 710 other hand, the analysis showed that the processing cost of  
 711 signaling represents the largest part of processing cost and  
 712 may constitute the system bottleneck.

## 713 Appendix A. Families of static threshold mechanisms

714 Each family can be represented by an increasing func-  
 715 tion  $F(x)$  defined in the interval  $0 < x < 1$ , with range from  
 716 0 to 1 and that is sampled at  $M$  equally spaced intervals  
 717 where  $M$  is the number of threshold levels. The threshold  
 718 values are equal to  $C \cdot F(k/M)$  where  $1 < k < M - 1$  and  
 719  $C$  is the link capacity. For example a linear function  
 720  $F(x) = x$  will define  $M$  equally spaced threshold level.

721 The first family that we have considered is a generaliza-  
 722 tion of the default threshold levels assumed in [25]. Accord-

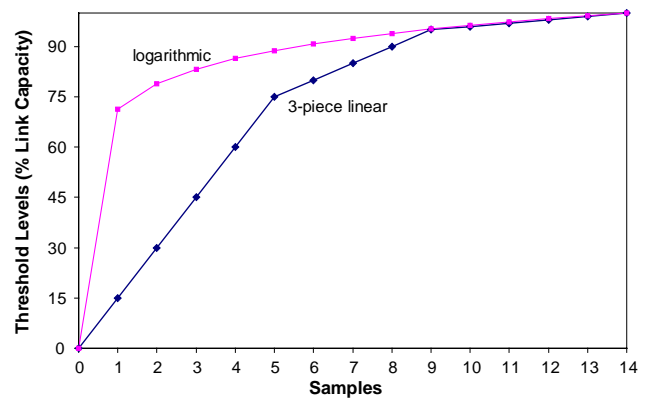


Fig. 16. Static threshold levels.

ing to [25], the threshold levels can be arbitrarily fixed while  
 the default is set to 14 levels. These 14 default levels actu-  
 ally define a 3-piece-linear function (see Fig. 16). We gener-  
 alize this function, assuming that each linear piece will  
 cover one third of the definition interval and considering  
 two parameters  $\beta$  and  $\gamma$  such that  $F(1/3) = \beta$  and  $F(2/3) = \gamma$   
 ( $0 < \beta < \gamma < 1$ ). A specific threshold setting for this  
 family is identified by  $(M, \beta, \text{ and } \gamma)$ . Therefore, there are  
 two degrees of freedom in adjusting the shape of the func-  
 tion to be sampled. The second family we considered is  
 based on a logarithmic function:  $F(x) = \ln(\alpha x)/\ln(\alpha)$ , with  
 $\alpha \gg M$ . The parameter  $\alpha$  defines the shape of the sampled  
 function, with small  $\alpha$  (e.g.,  $\alpha = 10^3$ ) the function will be  
 more similar to a linear function. For higher  $\alpha$  (e.g.,  
 $\alpha = 10^6$ ) there will be less detailed information when the  
 link is not loaded and much more precise information when  
 the link is heavily loaded. Using this “logarithmic”  
 mechanism, a specific choice of thresholds is identified by  
 $(M, \alpha)$ , i.e., we have a single parameter to change.

## Appendix B. Avoiding oscillations with static thresholds

The basic approach is to communicate the middle value  
 of an interval when a threshold is crossed [10]:  
 $L(k) = (F(k/N) + F((k+1)/N))/2$ . This may lead to  
 unneeded flooding when the bandwidth oscillates around  
 a threshold level. In [25] it is suggested to use different  
 increase and decrease thresholds to notify the increase  
 and the decrease of bandwidth occupancy, trying to avoid  
 this oscillation. The “increase” threshold  $F^+(k/N)$  and the  
 “decrease” threshold  $F^-(k/N)$  can be defined starting from  
 $F(k/N)$  as follows:

$$F^+(k/N) = F(k/N), \quad 754$$

$$F^-(k/N) = \frac{F(k/N) + F((k-1)/N)}{2}. \quad 756$$

On the other hand [25], considers to advertise the actual  
 value instead of a conventional value when a threshold is  
 crossed. When oscillating around a threshold value, for  
 example an increase threshold, a different status will be  
 communicated each time that the threshold is crossed in

762 the increase direction. Therefore, we decided to use the dif-  
763 ferent increase and decrease thresholds and to communi-  
764 cate the middle value as follow:

$$766 L^+(k) = (F^+((k+1)/N) + F^-(k/N))/2,$$

$$768 L^-(k) = (F^-(k/N) + F^+((k-1)/N))/2,$$

769 where  $L^+(k)$  and  $L^-(k)$  are the advertised level when the in-  
770 crease threshold  $F^+(k/N)$  and the decrease threshold  $F^-(k/N)$   
771 are crossed.

## 772 Appendix C. Number of messages for a flooding procedure

773 Let  $d_i$  be the degree of node  $i$ ,  $N$  be the number of nodes,  $D$   
774 be the average degree of a node; assume that originating  
775 node is  $n_1$ . The originating node will send  $d_1$  copies of the  
776 message. Each other node  $i$  will send  $d_i - 1$  copies (the node  
777 will not send the message on the receiving interface). Then:

$$\begin{aligned} \text{NumOfMsg} &= d_1 + \sum_{i=2}^N (d_i - 1) = 1 + \sum_{i=1}^N (d_i - 1) \\ &= 1 + \sum_{i=1}^N d_i - N = 1 + ND - N \\ 779 &= N(D - 1) + 1. \end{aligned}$$

## 780 References

- 781 [1] E. Rosen A. Viswanathan, R. Callon., Multiprotocol Label Switching  
782 Architecture, IETF RFC 3031, January 2001.  
783 [2] X. Xiao, A. Hannan, B. Bailey, L. M. Ni, Traffic Engineering with  
784 MPLS in the Internet", IEEE Network, March/April 2000.  
785 [3] D. Awduche et al., Requirements for Traffic Engineering Over MPLS,  
786 IETF RFC 2702, September 1999.  
787 [4] D. Katz, D. Yeung, K. Kompella, Traffic Engineering Extensions to  
788 OSPF Version 2, IETF RFC 3630, September 2003.  
789 [5] H. Smith, T. Li, IS-IS extensions for Traffic Engineering, IETF  
790 <draft-ietf-isis-traffic-04.txt>, IETF RFC 3784, June 2004.  
791 [6] D. Awduche, L. Berger, D. Gan, T. Li, V. Srinivasan, G. Swallow,  
792 RSVP-TE: Extensions to RSVP for LSP Tunnels, IETF RFC 3209,  
793 December 2001.

- [7] B. Jamoussi et al., Constraint-Based LSP Setup using LDP, IETF  
794 RFC 3212, January 2002. 795  
[8] L. Andersson, G. Swallow, The Multiprotocol Label Switching  
796 (MPLS) Working Group decision on MPLS signaling protocols,  
797 IETF RFC 3468, February 2003. 798  
[9] A. Shaikh, J. Rexford, K.G. Shin, Evaluating the Overheads of  
799 Source-Directed Quality-of-Service Routing", International Confer-  
800 ence on Network Protocols (ICNP), 1998. 801  
[10] G. Apostolopoulos, R. Guerin, S. Kamat, S.K.Tripathi, Quality of  
802 Service Based Routing: A Performance Perspective, SIGCOMM  
803 1998. 804  
[11] G. Apostolopoulos, R. Guerin, S. Kamat, Implementation and  
805 Performance Measurements of QoS Routing Extensions to OSPF,  
806 Infocom, 1999. 807  
[12] R.R. Irashko, W.D. Grover, M.H. MacGregor, Optimal capacity  
808 placement for path restoration in STM or ATM mesh-survivable  
809 networks, IEEE/ACT Trans. on Networking, June 1998. 810  
[13] A. Basu, J.G. Riecke, Stability Issues in OSPF Routing", SIG-  
811 COMM, 2001. 812  
[14] G. Conte, P. Iovanna, R. Sabella, M. Settembre, L. Valentini, A  
813 Traffic Engineering Solution for GMPLS Network: A Hybrid  
814 Approach Based on Off-line and On-line Routing Methods, ONDM  
815 2003 Conference, February 4-6, 2003 Budapest, Hungary. 816  
[15] MPLS-TE control plane simulator <[http://www.coritel.it/  
817 download.html](http://www.coritel.it/download.html)>. 818  
[16] Sourceforge MPLS home page, <<http://mpls-linux.sourceforge.net/>>. 819  
[17] IBCN testlab Home Page <<http://dsmpls.atlantis.rug.ac.be/>>. 820  
[18] Zebra Home Page, <<http://www.zebra.org/>>. 821  
[19] J. Moy, OSPF Version 2, IETF RFC 2328, April 1998. 822  
[20] R. Coltun, The OSPF Opaque LSA option, IETF RFC 2370, July  
823 1998. 824  
[21] A. Bosco, A. Botta, M. Intermite, P. Iovanna, S. Salsano, Distributed  
825 Implementation of a Pre-Emption and Re-routing Mechanisms for a  
826 Network Control Based on IP/MPLS Paradigm, ONDM 2003  
827 Conference, February 4-6, 2003 Budapest, Hungary. 828  
[22] A. Bosco, A. Botta, G. Conte, P. Iovanna, R. Sabella, S. Salsano,  
829 Internet like control for MPLS based traffic engineering: performance  
830 evaluation, Performance Evaluation, vol. 59/2-3, February 2005,  
831 Elsevier Science, pp 121-136. 832  
[23] A. Shaikh, A. Greenberg, Experience in Black-box OSPF Measure-  
833 ment, ACM SIGCOMM Internet Measurement Workshop (IMW),  
834 November 2001. 835  
[24] K. Nemeth, G. Feher, I. Cseleny, Benchmarking of Signaling  
836 Based Resource Reservation in the Internet", Networking  
837 2000. 838  
[25] CISCO on line documentation: "MPLS Traffic Engineering". 839  
840